Fibers and Polymers 2006, Vol.7, No.4, 333-338

Structural and Physical Properties of *Antheraea pernyi* Silk Fibroin Fiber Treated with I_2-KI Aqueous Solution

Md. Majibur Rahman Khan, Yasuo Gotoh, Hideaki Morikawa*, and Mikihiko Miura

Faculty of Textile Science and Technology, Shinshu University, Ueda, Nagano 386-8567, Japan
(Received August 16, 2006; Revised October 4, 2006; Accepted October 23, 2006)

Abstract: Silk fibroin (SF) fiber from the *Antheraea pernyi* silkworm was treated with a 1.23 N iodine-potassium iodide (I_2-KI) aqueous solution, and the structure and physical properties were investigated to clarify the effects of the iodine treatment. The noticeably high weight gain value of SF fiber, about 25 wt% was attributed to the absorption of polyiodide ions in the form of I_3^- and I_5^-. Fourier transform infrared spectroscopy and X-ray diffraction measurements suggested that polyiodide ions mainly entered the amorphous region. In addition, a new sharp reflection on the meridional direction, corresponding to a period of 7.0 Å, was observed and indicated the possibility of the formation of mesophase structure of β-conformation chains. Dynamic viscoelastic measurements showed that the damping tan δ peak at 270 °C gradually shifted to lower temperature in the iodinated SF fibers, suggesting an enhancement of the molecular motion of the fibroin chains induced by the presence of polyiodide ions. With heating above 254 °C, the iodine component introduced intermolecular cross-linking of SF, and the melt flow of the sample was inhibited. The thermal decomposition stability of fibroin molecules was greatly enhanced by iodine treatment.

Keywords: *Antheraea pernyi* silk fibroin, Iodine treatment, Structure, Molecular motion, Thermal properties

Introduction

Since the dawn of human civilization, the silkworm has been used as a source of silk for producing exquisite textiles and dress materials. A wide range of silk spinning insects exists in nature, including caterpillars and spiders. Among the silkworm species, silk from the domesticated silkworm, *Bombyx mori* (*B. mori*) is commonly used, and tussah silk, the silk fiber from wild silkworm, *Antheraea pernyi* (*A. pernyi*), has been used as textile materials as a variation to domestic silkworm silk.

Several studies have been performed on the chemical structure, molecular conformation and physical properties of *A. pernyi* silk fibroin (SF) fiber [1-6]. The chemical composition of *A. pernyi* SF is significantly different from that of *B. mori* SF. The alanine content is higher than that of glycine and the composition is related to the abundance of $-(Ala)_n-$ sequence, which favors α-helix formation [7]. Furthermore, the amount of basic (lysine, histidine and arginine) and acidic (aspartic and glutamic acid) amino acid residues of *A. pernyi* SF is considerably higher. It also contains certain amount of tri-peptide sequence, Arg-Gly-Asp, which is known to exhibit specific interactions with mammal cells, favors their attachment in biomedical uses [8-10]. Based on these features, the study of the physico-chemical properties and structure performance of *A. pernyi* SF has been recently stimulated by the increasing demand of new high performing, environmentally friendly, and futuristic materials for a wide range of advanced biotechnological and biomedical applications such as tissue engineering matrix [9], cell culture substrate [10], surgical suture [11], enzyme immobilization membrane [12] and soft contact lenses [13].

To diversify the textile and non-textile products of tussah SF fibers, physico-chemical treatment, and polymer-alloying or blending with other polymers are necessary to improve their inferior properties. Among the many investigations that have been reported, aqueous methanol treatment [14], chemical cross-linking with PEG-DE [15], chemical treatment with epoxides [16], NaOH [17], acid anhydrides [18], stannic acid [19], polymer-alloying by graft copolymerization [20], blending with chitosan [21], poly acrylic acid [22], *B. mori* SF [23] are included.

Iodine is one of five non-metallic elements called halogens. Halogens readily share electrons in covalent bonds with other atoms to complete an octet of electrons in their valence shell. Of the many modification techniques for polymers, iodine treatment causes antibacterial properties. For example, iodinated cadexomer, a polysaccharide including iodine, is applied to a pharmaceutical material as a wound healing medicine, due to its high antibacterial activity [24]. Iodine molecules can form complexes with many kinds of polymers such as nylon 6 [25], starch [26], poly(vinyl alcohol) [27], and chitosan [28] etc.

In connection with the iodine treatment of SF, we previously reported that iodine treatment has greatly influenced the molecular structure and properties of *B. mori* SF [29]. The results of iodine sorption experiment performed on *B. mori* SF were characterized by a new sharp reflection on the meridional direction, corresponding to a period of 7.0 Å. We described a mesophase model to explain this new meridional peak. Therefore, some changes of structure and property can be expected for iodine treatment of *A. pernyi* SF that contributes to produce new materials with selected functional properties. The action of iodine into tussah SF has been investigated [30].

*Corresponding author: morikaw@shinshu-u.ac.jp

However, extensive investigations have been very limited and until recently little attention has been paid to the characterization of the structure and properties of iodinated *A. pernyi* SF.

The aim of this study is to investigate the effects of iodine treatment on the structure and properties of *A. pernyi* SF fiber using X-ray diffraction (XRD), Fourier transform infrared (FT-IR) spectroscopy, dynamic mechanical thermal analysis (DMTA), thermogravimetric (TG) analysis, and tensile measurements.

Experimental

Materials

A. pernyi cocoon fiber provided by North Eastern Industrial Research Center, Shiga prefecture, Japan was first degummed to remove sericin. The degumming process was performed by standard marseille soap/soda ash method [31].

Iodine Treatment

At first, a 1.23 N iodine-potassium iodide (I_2-KI) aqueous solution was prepared in a tube and kept about 24 h at room temperature with gentle stirring to dissolve iodine into potassium iodide properly. The degummed *A. pernyi* SF fibers were wound in a teflon plate (80 mm length) to constrain fiber length and immersed in the 1.23 N I_2-KI aqueous solution at laboratory atmosphere, 25 °C and 65 % relative humidity (RH). To investigate the saturated point of iodine absorption, fiber was treated for various periods. After each immersion period, the fiber was sufficiently rinsed with distilled water and dried in an electric oven at 95 °C for 3 h.

Weight Gain

Fiber weight gain, I_t, by absorption of iodine component (including potassium ions as a counter ion) was calculated from the difference in weight of the fiber before and after iodine treatment according to the following equation:

$$I_t = \frac{I_2 - I_1}{I_1} \times 100$$

where I_1 and I_2 are the weights of the dried fiber before and after the immersion in the I_2-KI solution, respectively.

Measurements

FT-IR spectroscopy was measured with a Shimadzu FT-IR-8400S in the region of 4000~400 cm^{-1} at room temperature. The fibers were crushed in liquid nitrogen and then examined in KBr discs.

An XRD photograph was taken with the microbeam X-ray at beam line BL40B2 with a wavelength of 1.0 Å at 8 keV of synchrotron radiation at SPring-8 (Harima, Japan).

A wide angle X-ray diffraction (WAXD) profile was obtained with a Rigaku Rotorflex RU-200B diffractometer with Ni-filtered CuK_α radiation generated at 40 kV and 150 mA.

DMTA was measured with an ITK Co. DVA-225 at a stretching mode of 10 Hz and at a heating rate of 10 °C min^{-1} on fibers of 20 mm length.

TG analysis was carried out with a Rigaku Thermo plus TG 8120 under N_2 gas at a scanning rate of 10 °C min^{-1}.

The tensile properties were measured with a Tensilon Model RTC 1250A, (Orientec Corporation), Japan using standard technique at 22 °C and 65 %RH at a gauge length of 40 mm and strain rate of 40 mm/min. The experimental results represent the average of 20 individual measurements.

Results and Discussion

Iodine Absorption Behavior

Figure 1 shows the weight gain of *A. pernyi* SF fibers by immersion in I_2-KI solution plotted against the treatment time. By iodine absorption, the weight gain is increased rapidly with immersion time and is saturated at around 25 wt% until at least 162 h. On the other hand, by absorbing polyiodide ions (I_3^- and I_5^-), the weight gain of *B. mori* SF was linearly increased and was saturated at about 20 wt% after an immersion time of 40 h [29]. Amino acid composition and structural characteristics of *A. pernyi* SF are different from those of *B. mori* SF. Therefore iodine absorption behavior is expected to be different between them. Comparatively higher iodine-absorption power of *A. pernyi* SF seems to be related to a difference in the higher-order structures, and abundant of the amount of basic and acidic amino acid residues in tussah SF molecules.

FT-IR Spectra

Since the position and intensity of amide bands are sensitive to molecular conformation of fibroins, FT-IR spectroscopy seems to be a powerful technique to study the molecular conformation and crystalline structure of silk protein. Figure 2 shows FT-IR spectra of untreated and iodinated *A. pernyi* SF fibers. The spectrum of untreated specimen shows a

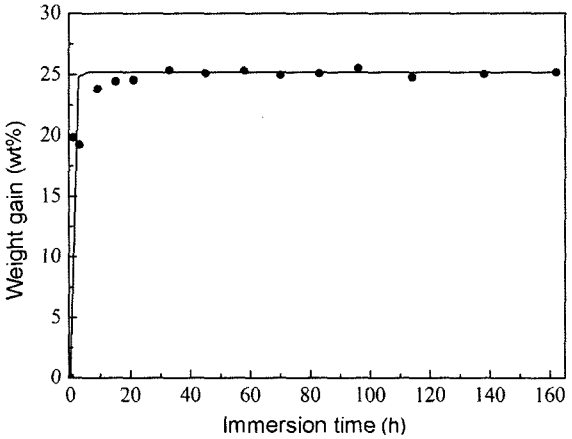

Figure 1. Weight gain of *A. pernyi* SF fibers by immersion in a 1.23 N I_2-KI solution at different immersion times.

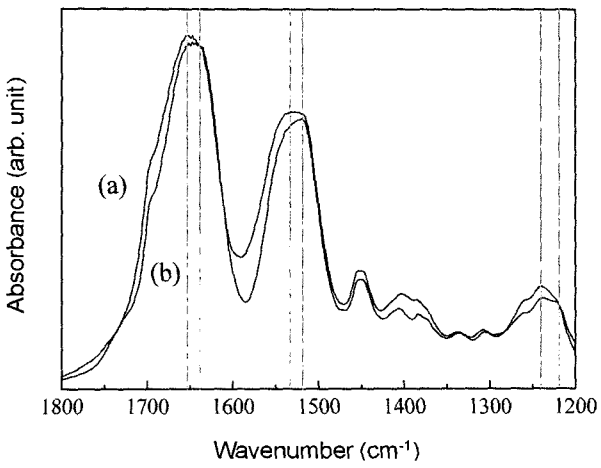

Figure 2. FT-IR spectra of *A. pernyi* SF fibers treated with a 1.23 N I_2-KI solution for 162 h; (a) untreated specimen and (b) iodinated specimen.

strong absorption band at 1652 cm^{-1} (amide I), attributed to the α-helix conformation, 1535 cm^{-1} (amide II), intermediate position between α-helix and β-sheet structure, and 1238 cm^{-1} (amide III), β-sheet structure [15,32]. On the other hand, iodinated specimen shows strong absorption band at 1638 cm^{-1} (amide I), 1519 cm^{-1} (amide II), and a new peak at 1218 cm^{-1} (amide III), assigned to the β-sheet conformation [21,32]. This result indicates that the introduction of polyiodide ions increases the β-structure content of SF molecules.

XRD Photographs

Figure 3 shows XRD photographs of untreated and iodinated tussah SF fibers. Untreated specimen, shows a typical diffraction pattern of *A. pernyi* SF as reported as Tsukada *et al.* [16]. After iodine treatment, the diffraction pattern becomes comparatively ambiguous, and a new reflection appears in the meridional direction as indicated with an arrow, which corresponds to d-spacing of 7.0 Å. After iodination of *B. mori* SF, the same reflection appeared in the meridional direction corresponding to 7.0 Å and we explained this new

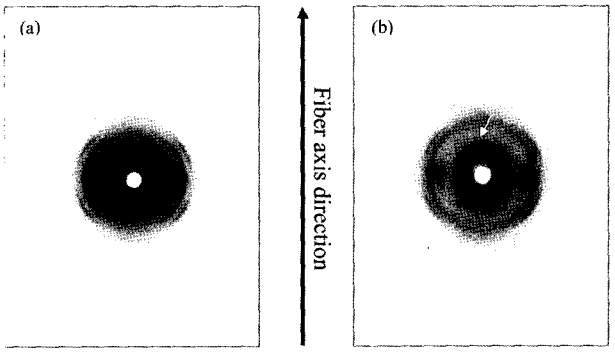

Figure 3. XRD photographs of *A. pernyi* SF fibers treated with a 1.23 N I_2-KI solution for 162 h; (a) untreated specimen and (b) iodinated specimen.

reflection by defining a model that indicates the possibility of formation of mesophase structure of β-conformation chains [29]. Polyiodide ions are introduced mainly into the amorphous regions of SF fiber and cause to weak the hydrogen bonding between amide groups. As a result, molecular chains in amorphous state is relaxed, consequently the orientation of the crystallites is decreased. At the same time, the relaxed molecular chains of the amorphous regions can move more easily, and a part of them transform to the mesophase structure.

WAXD Profiles

Equatorial WAXD profiles of untreated and iodinated *A. pernyi* SF fibers are shown in Figure 4. From Figure 4(a), untreated specimen shows diffraction peaks at about 16.7° (lattice spacing, d = 5.30 Å), and 20.3° (d = 4.37 Å) attributed to the typical β-sheet structure, and a minor peak at 24.0° corresponding to d-spacing 3.70 Å, assigned to a-helix structure of tussah SF fiber [32]. After iodine treatment, the intensity of major two peaks (corresponding to 5.30 Å and 4.37 Å) becomes much smaller as shown in Figure 4(b), which is mainly attributed to both the large X-ray absorption coefficient of iodine and the decrease in the crystallite orientation. On the other hand, the positions of the diffraction peaks are unchanged after iodination (The peak positions were corrected by using silicon powder), only the minor peak (d = 3.70 Å) does not appeared. It is to mention here that the small sharp peak at 25.4° is appeared from KI (potassium iodide). So there is no relation between SF crystal peak and the sharp peak at 25.4°. These results indicate that the crystal form of SF can be basically identified as β-sheet structure, and this crystal form is retained after the iodine treatment.

Dynamic Viscoelastic Properties

DMTA is known as a sensitive method of monitoring the

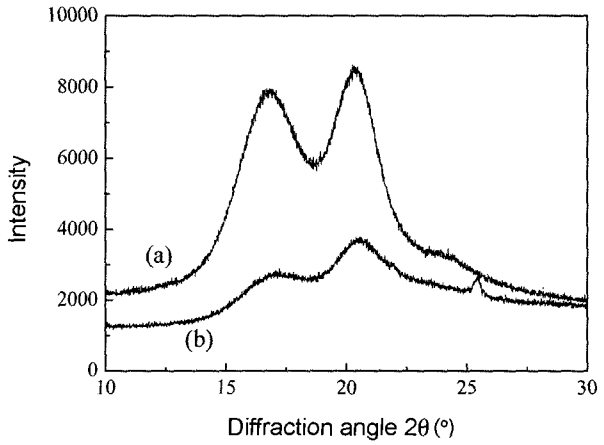

Figure 4. Equatorial WAXD profiles of *A. pernyi* SF fibers treated with a 1.23 N I_2-KI solution for 162 h; (a) untreated specimen and (b) iodinated specimen. The profiles were measured with the reflection method, and the same quantity of each sample was coated with silicon powder for angle calibration.

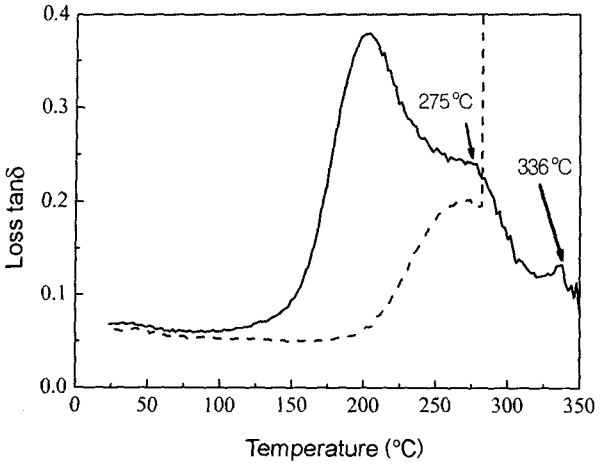

Figure 5. Temperature dependence of tanδ for *A. pernyi* SF fibers treated with a 1.23 N I_2-KI solution for 162 h; (dotted line ------) untreated specimen and (solid line ——) iodinated specimen.

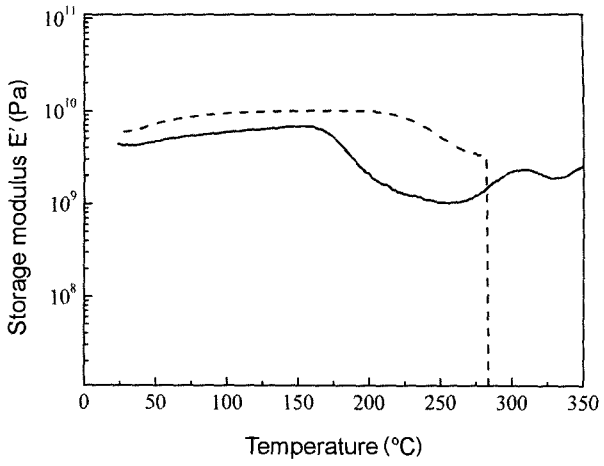

Figure 6. Temperature dependence of storage modulus for *A. pernyi* SF fibers treated with a 1.23 N I_2-KI solution for 162 h; (dotted line -----) untreated specimen and (solid line ——) iodinated specimen.

side/main-chain motion in specific regions and local mode relaxations of the silk protein. The dynamic storage modulus (E') and mechanical damping tan δ of iodinated tussah SF fibers were examined.

Figure 5 shows temperature dependence of mechanical damping tan δ for untreated and iodinated *A. pernyi* SF fibers. The untreated specimen displays the onset of an increase in tan δ at 172 °C and a prominent relaxation peak at 270 °C. This is due to the molecular motion in the crystals of *A. pernyi* SF fiber [33]. After iodination, the damping tan δ peak increases abruptly at about ca. 100 °C and reaches a maximum relaxation at ca. 203 °C, which is ca. 67 °C lower than that of untreated specimen. The magnitude of maximum relaxation peak is much higher. This behavior is primarily attributed to ease the molecular motion of fiber molecules by reaction of iodine component with SF molecules. The iodine component weakens the hydrogen bonding between the molecules forming the β-sheets, and contributes to the enhancement of molecular motion of crystals with heating. This result is in good agreement with the decrease in WAXD intensity described in preceding paragraph.

The damping tan δ peaks of iodinated *A. pernyi* SF are characterized by two minor onsets observed at 275 and 336 °C respectively. Though the origin of these relaxations has not been determined, but these are most likely related to molecular motion of the cross-linked SF molecules. The evidence of the cross-linking of SF will be shown in the next figure.

The temperature dependence of the storage modulus (E') for untreated and iodinated *A. pernyi* SF fiber is shown in Figure 6. The storage modulus of untreated specimen increases gradually with temperature up to 127 °C, owing to the evaporation of moisture contained in the fiber. The E' curve then remains stable until about ca. 202 °C, followed by a sharp decrease as a consequence of the higher thermal movement of fibroin chains attributed to the weakening of the intermolecular interactions. The second plateau of the E' curve is shown between ca. 220-281 °C, and then E' exhibits a sharp fall around 281 °C, due to melting of the crystallites.

On the other hand, The E' curve of iodinated *A. pernyi* SF shows that the thermal stability of fibers decreased significantly by introduction of polyiodide ions into fibers. Initially, the iodinated specimen exhibits an E' curve similar to that of untreated one, with a smaller E' value, except above 254 °C. The first fall of onset temperature is shifted to lower temperature at ca. 159 °C than that observed for the untreated specimen at ca. 202 °C. These changes of E' behavior may be attributed to the effect of introduction of polyiodide ions into fiber segments, which remained within the fiber matrix long enough causes SF molecular motion to occur more easily with heat, and consequent softening of the SF molecules.

Above 254 °C, the iodinated specimen shows the increase of E' restricting the melt-flowing of fibers and the onset exhibits at 308 °C. After decreasing to 329 °C, the E' curve again starts to increase. The onset in higher temperature of iodinated SF implies the formation of intermolecular cross-linking of fibroin molecules accompanied by a hardening of the sample. Although the reason for the formation of cross-linking has not yet been determined, it is most likely related to the iodine component.

Thermal Properties

The thermal behavior of iodinated tussah SF fiber was investigated using TG methods. Figure 7 shows the TG and differential thermogravimetric (DTG) curves for both untreated and iodinated *A. pernyi* SF fibers.

For untreated specimen, the initial weight loss below 120 °C is attributed to the evaporation of water, and is followed by nearly constant weight from 110 to 210 °C. With increasing temperature, the thermal decomposition is proceeded step by

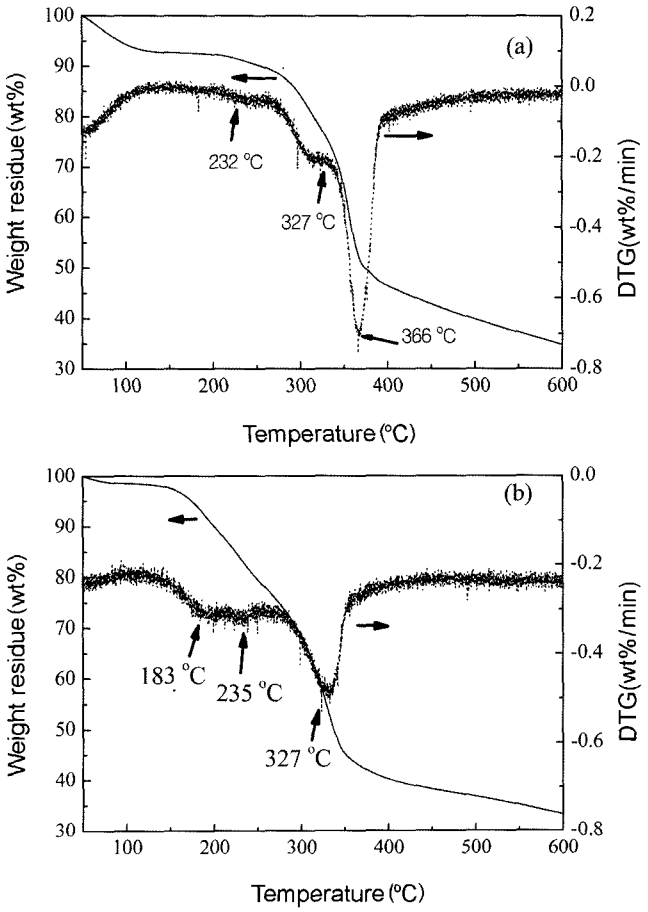

Figure 7. TG and DTG curves of *A. pernyi* SF fibers treated with a 1.23 N I_2-KI solution for 162 h; (a) untreated specimen and (b) iodinated specimen.

step, depending on a certain temperature range. According to TG results, thermal decomposition of untreated specimen exhibits three main decomposition stages: the first step, a minor thermal decomposition of SF takes place in the temperature range from 210 to 320 °C; the second, a drastic decomposition step from 320 to 370 °C; and the third, from 370 to 400 °C. These decompositions are associated with the degradation of side chain groups of amino acid residues and the cleavage of peptide bonds of *A. pernyi* SF fiber [34]. The differential weight loss (dW/dT), DTG curves provide clear evidence for the above three degradation steps. The maximum degradation temperature of each step is obtained about 232, 327, and 366 °C, respectively.

On the other hand, the thermal decomposition behavior of *A. pernyi* SF fiber is significantly influenced by iodine treatment. In TG curve, the iodinated specimen shows that the decomposition in different steps is shifted to lower temperature: the first decomposition shifts to 120-160 °C; second step 160-300 °C; and third step 300-347 °C. Accordingly in DTG curve, the maximum degradation of each step in iodinated specimen is shifted at about 183, 235, and 327 °C

Table 1. Tensile properties of *A. pernyi* SF fibers treated with a 1.23 N I_2-KI solution for 162 h

Sample	Strength (g/d)	Elongation (%)
Untreated SF fiber	2.7	31.1
Iodinated SF fiber	2.5	26.7

respectively. These results should be related to not only degradation of SF, but also vaporization of the iodine component in the specimen, because of ca. 25 wt% of polyiodide ions are included in the specimen, and evaporation of most of the iodine component was confirmed during the TG measurement. Above 400 °C, the TG curve trend for each sample is almost similar and coincident at about 600 °C. Since the initial weight of the iodinated specimen contains an iodine component of 25 wt%, it can be said that the final residual carbon weight would be higher than that of the untreated one. This may be related to the intermolecular cross-linking of SF by iodination, which may cause inhibition of volatile component containing carbon from SF during heating and lead to higher carbon yield.

Tensile Properties

Tensile properties, particularly tensile strength and elongation% are the most important factors for evaluating the performance of fibers for proper applications. Table 1 illustrates the tensile strength and elongation% of both untreated and iodinated *A. pernyi* SF fibers. It can be observed that the variation of tensile strength is very small, suggesting that iodine treatment does not have a significant effect on the intrinsic tensile properties. Only the elongation value, 31.1 % in the dry state decreased to 26.7 % with introduction of iodine ions into SF molecules. These results can be explained by not only associated with hydrozen-bond loosening or partial breakage as long as peptide bond formation but also the increase of fiber size associated with swelling behavior of the iodinated SF fibers.

Conclusion

To elucidate the effects of iodine treatments on SF fiber, the structure and properties of *A. pernyi* SF fibers treated with 1.23 N I_2-KI aqueous solutions were investigated with FT-IR, XRD, DMTA, TG and tensile measurements. The weight gain of iodinated *A. pernyi* SF fibers was 25 wt%, which was comparatively higher than that of *B. mori* SF (*cf.* weight gain was 20 wt% for *B. mori* SF). This reason is considered to be related to a difference in the higher-order structures between *B. mori* SF and *A. pernyi* SF fibers. FT-IR and XRD measurements suggested that polyiodide ions mainly entered the amorphous region. Moreover, a new sharp reflection on the meridional direction, corresponding to a period of 7.0 Å was observed, which indicates the possibility of formation of mesophase structure of β-conformation chains.

DMTA measurements showed that the molecular motion of the crystalline regions at 270 °C was enhanced and shifted to lower temperature by the introduction of polyiodide ions. This indicates that the iodine component weakens the hydrogen bonding between SF molecules forming the β-sheet structure, and causes molecular motion of the crystal to occur more easily with heating. With heating above 254 °C, the iodine component introduced intermolecular cross-linking of SF, and the melt flow of the sample was inhibited. TG measurements indicated that the thermal decomposition stability of fibroin molecules was greatly enhanced by introduction of polyiodide ions into SF molecules. Iodinated *A. pernyi* SF fibers did not show a significant effect on the intrinsic tensile properties.

Acknowledgements

The authors wish to express their thanks to the North Eastern Industrial Research Center, Shiga prefecture, Japan, for kindly supplying the SF fibers. The authors also acknowledge the support of a Grant-in-Aid from the Center of Excellence for 21st Century Research program of the Ministry of Education, Culture, Science and Technology of Japan. The synchrotron radiation experiments were performed at the BL40B2 in the SPring-8 with the approval of the Japan Synchrotron Radiation Research Institute (JASRI) (Proposal No. 2005B0366).

References

1. R. E. Marsh, R. B. Corey, and L. Pauling, *Acta Cryst.*, **8**, 710 (1955).
2. G. Freddi and M. Tsukada, *Current Trends in Polym. Sci.*, **5**, 53 (2000).
3. M. Tsukada, G. Freddi, Y. Gotoh, and N. Kasai, *J. Polym. Sci. Part-B: Polym. Phys.*, **32**, 1407 (1994).
4. Y. Kawahara, T. Hananouchi, and T. Kimura, *Text. Res. J.*, **73**, 289 (2003).
5. F. Lucas, J. T. B. Shaw, and S. G. Smith, *J. Mol. Biol.*, **2**, 339 (1960).
6. J. Kirimura, M. Saito, and M. Kobayashi, *Nature*, **195**, 729 (1962).
7. J. T. B. Shaw and S. G. Smith, *Biochem. Biophys. Acta*, **52**, 305 (1961).
8. M. D. Pierschbacher and E. Ruoslahti, *Nature*, **309**, 30 (1984).
9. M. D. Pierschbacher and E. Ruoslahti, *Proc. Natl. Acad. Sci. USA*, **81**, 5985 (1984).
10. N. Minoura, S. Aiba, M. Higuchi, Y. Gotoh, M. Tsukada, and Y. Imai, *Biochem. Biophy. Res. Commun.*, **208**, 511 (1995).
11. G. N. Gapurova, *Zdravookhranenie Turkmenistana*, **27**, 15 (1983).
12. Y. Kawahara, *J. Seric. Sci. Jpn.*, **62**, 272 (1993).
13. T. Tsuruta, T. Hayashi, K. Kataoka, K. Ishihara, and Y. Kimura in "Biomedical Applications of Polymeric Materials", p.128, CRC Press, Boca Raton, FLXS, 1993.
14. H. Y. Kweon and Y. H. Park, *J. Appl. Polym. Sci.*, **73**, 2887 (1999).
15. M. Li, W. Tao, S. Lu, and S. Kuga, *Int. J. Biol. Macromol.*, **32**, 159 (2003).
16. M. Tsukada, Y. Gotoh, G. Freddi, M. Matsumura, H. Shiozaki, and H. Ishikawa, *J. Appl. Polym. Sci.*, **44**, 2203 (1992).
17. G. Freddi, H. Kato, M. Tsukada, G. Allara, and H. Shiozaki, *J. Appl. Polym. Sci.*, **55**, 481 (1995).
18. M. Tsukada, T. Arai, and S. Winkler, *J. Appl. Polym. Sci.*, **78**, 382 (2000).
19. Y. Kawahara and M. Shioya, *J. Appl. Polym. Sci.*, **73**, 363 (1999).
20. M. Tsukada, G. Freddi, M. R. Massafra, and S. Beretta, *J. Appl. Polym. Sci.*, **67**, 1393 (1998).
21. H. Y. Kweon, I. C. Um, and Y. H. Park, *Polymer*, **42**, 6651 (2001).
22. Q. Peng, Q. Xu, H. Xu, M. Pang, J. Li, and D. Sun, *J. Appl. Polym. Sci.*, **98**, 864 (2005).
23. M. Tsukada, G. Freddi, and N. Kasai, *J. Polym. Sci. Part-B: Polym. Phys.*, **32**, 1175 (1994).
24. H. Akiyama, T. Oono, M. Saito, and K. Iwatsuki, *J. Dermatol.*, **31**, 529 (2004).
25. A. Kawaguchi, *Polymer*, **33**, 3981 (1992).
26. A. Cesàro and D. A. Brant, *Biopolymers*, **16**, 983 (1997).
27. J. H. Yeum, J. W. Kwak, S. S. Han, S. S. Kim, B. C. Ji, S. K. Noh, and W. S. Lyoo, *J. Appl. Polym. Sci.*, **94**, 1435 (2004).
28. H. Yajima, M. Morita, M. Hashimoto, H. Sashiwa, T. Kikuchi, and T. Ishii, *Int. J. Thermophys.*, **22**, 1265 (2001).
29. M. M. R. Khan, Y. Gotoh, M. Miura, H. Morikawa, and M. Nagura, *J. Polym. Sci. Part-B: Polym. Phys.*, **44**, 3418 (2006).
30. H. Lecus, *Angew. Chem.*, **47**, 779 (1934).
31. H. Kato in "Silk Processing Techniques and its Application", pp.18-19, Elsevier, Amsterdam, 1968.
32. M. Li, W. Tao, S. Kuga, and Y. Nishiyama, *Polym. Adv. Technol.*, **14**, 694 (2003).
33. M. Nagura in "Structure of Silk Yarn Part –A: Biological and Physical Aspects", Topics on "Molecular Motion in Silk Fibre", p.249, Science Publishers Inc., UK, 2000.
34. G. Freddi, M. Tsukada, and S. Beretta, *J. Appl. Polym. Sci.*, **71**, 1563 (1999).